

## Accurate measurements of fission-fragment yields in $^{234,235,236,238}\text{U}(\gamma, f)$ with the SOFIA set-up

A. Chatillon, J. Taïeb, J.-F. Martin, E. Pellereau, G. Boutoux, T. Gorbinet, L. Grente, G. Bélier, B. Laurent, H. Alvarez-Pol, et al.

### ► To cite this version:

A. Chatillon, J. Taïeb, J.-F. Martin, E. Pellereau, G. Boutoux, et al.. Accurate measurements of fission-fragment yields in  $^{234,235,236,238}\text{U}(\gamma, f)$  with the SOFIA set-up. Fourth International Workshop on Nuclear Data Evaluation for Reactor Applications (WONDER-2015), Oct 2015, Aix en Provence, France. pp.08001, 10.1051/epjconf/201611108001 . in2p3-01291181

**HAL Id: in2p3-01291181**

**<http://hal.in2p3.fr/in2p3-01291181>**

Submitted on 21 Mar 2016

**HAL** is a multi-disciplinary open access archive for the deposit and dissemination of scientific research documents, whether they are published or not. The documents may come from teaching and research institutions in France or abroad, or from public or private research centers.

L'archive ouverte pluridisciplinaire **HAL**, est destinée au dépôt et à la diffusion de documents scientifiques de niveau recherche, publiés ou non, émanant des établissements d'enseignement et de recherche français ou étrangers, des laboratoires publics ou privés.

## Accurate measurements of fission-fragment yields in $^{234,235,236,238}\text{U}(\gamma, f)$ with the SOFIA set-up

A. Chatillon<sup>1,a</sup>, J. Taïeb<sup>1</sup>, J.-F. Martin<sup>1</sup>, E. Pellereau<sup>1</sup>, G. Boutoux<sup>1</sup>, T. Gorbine<sup>1</sup>, L. Grente<sup>1</sup>, G. Bélier<sup>1</sup>, B. Laurent<sup>1</sup>, H. Alvarez-Pol<sup>2</sup>, Y. Ayyad<sup>2</sup>, J. Benlliure<sup>2</sup>, M. Caamaño<sup>2</sup>, L. Audouin<sup>3</sup>, E. Casarejos<sup>4</sup>, D. Cortina-Gil<sup>2</sup>, F. Farget<sup>5</sup>, B. Fernández-Domínguez<sup>2</sup>, A. Heinz<sup>6</sup>, B. Jurado<sup>7</sup>, A. Kelić-Heil<sup>8</sup>, N. Kurz<sup>8</sup>, S. Lindberg<sup>6</sup>, B. Löher<sup>8</sup>, C. Nociforo<sup>8</sup>, C. Paradela<sup>2</sup>, S. Pietri<sup>8</sup>, D. Ramos<sup>2</sup>, J.-L. Rodríguez-Sánchez<sup>2</sup>, C. Rodríguez-Tajes<sup>5</sup>, D. Rossi<sup>8</sup>, K.-H. Schmidt<sup>8</sup>, H. Simon<sup>8</sup>, L. Tassan-Got<sup>3</sup>, H. Törnqvist<sup>9</sup>, J. Vargas<sup>2</sup>, B. Voss<sup>8</sup>, H. Weick<sup>8</sup>, and Y. Yan<sup>3</sup>

<sup>1</sup>CEA, DAM, DIF, F-91297 Arpajon, France

<sup>2</sup>Dpt. of Particle Physics, University of Santiago de Compostela, E-15782 Santiago de Compostela, Spain

<sup>3</sup>Institut de Physique Nucléaire d'Orsay, Université Paris-Sud, CNRS, IN2P3, 91406 Orsay, France

<sup>4</sup>University of Vigo, E-36310 Vigo, Spain

<sup>5</sup>CNRS, GANIL, Bd. H. Becquerel, 14076 Caen, France

<sup>6</sup>Chalmers University of Technology, 41296 Gothenburg, Sweden

<sup>7</sup>CNRS, CENBG, F-33175 Gradignan, France

<sup>8</sup>GSI, Planckstr. 1, 64291 Darmstadt, Germany

<sup>9</sup>Institut für Kernphysik, Technische Universität Darmstadt, 64289 Darmstadt, Germany

**Abstract.** SOFIA (Studies On Fission with Aladin) is a new experimental set-up dedicated to accurate measurement of fission-fragments isotopic yields. It is located at GSI, the only place to use inverse kinematics at relativistic energies in order to study the  $(\gamma, f)$  electromagnetic-induced fission. The SOFIA set-up is a large-acceptance magnetic spectrometer, which allows to fully identify both fission fragments in coincidence on the whole fission-fragment range. This paper will report on fission yields obtained in  $^{234,235,236,238}\text{U}(\gamma, f)$  reactions.

## 1 Introduction

Data on fission-fragment yields are still up to now incomplete and often inaccurate despite decades of advanced investigations. Even for the most studied reaction, i.e., thermal-neutron-induced fission of  $^{235}\text{U}$ , uncertainties attached to isotopic fission yields are mainly above 30 % [1]. This lack of high-resolution data constitutes an obstacle to the development of predictive and reliable models, and yet, accurate yields data of isotopic fission fragments are crucial for nuclear-reactor applications, to simulate the nuclear fuel burn-up associated with the accumulation of fission products in the core, the neutron flux, or, the decay heat after a core shutdown.

---

<sup>a</sup>e-mail: audrey.chatillon@cea.fr

## 1.1 Experimental limitations due to direct kinematics

Experimental constraints in direct kinematics, where a neutron, light charged particle or  $\gamma$  beam impinges on an actinide target, prevent from measuring unambiguously the mass and the nuclear charge of the fission fragments especially for the heavy group. From radiochemical methods, high-resolution data of fission-product isotopic yields, after  $\beta$ -decay, can be obtained but only for few nuclei [2]. From physical methods, ionic charge states and masses can be respectively deduced from the energy-loss and total energy measurements. The nuclear-charge identification is then limited to the light fragments [3–5] due to the strong fluctuation of ionic charge states preventing a clear assignment of the atomic number in the heavy group. Moreover, fission fragments having a low recoil energy, their energy straggling in dead layers limits the resolution to  $\sigma \sim 1.5$  MeV [6]. Therefore the mass resolution is around 4 mass unit (FWHM). With the advent of recoil spectrometers, such as Lohengrin [7] or Hiawatha [8], high-resolution data on isobaric yields are finally reached with an uncertainty below 5%. But still, isotopic identification is limited to the light group, for example Refs. [9–11], except during experiments where  $\beta$ -delayed  $\gamma$ -rays are measured [12]. This latter method allows to measure only some isotopic yields in the heavy group, and results on isotopic yields remain partial.

## 1.2 An alternative approach: Surrogate reactions using inverse kinematics

A new generation of experiments based on inverse kinematics coupled with a spectrometer has been developed. Actinides are accelerated, and the compound nuclei are produced using surrogate reactions. Thanks to the kinematical boost, fission fragments are emitted at forward angles with a higher recoil energy, and their elemental distribution is measured with an improved resolution. Using this technique, isotopic yields are reachable even for the heavy group.

At GANIL, inverse kinematics is used to produce fissioning nuclei by transfer or fusion reactions of  $^{238}\text{U}$  beam at 6 A.MeV on a  $^{12}\text{C}$  target [13]. In this experiment, the VAMOS spectrometer [14] is used to isotopically identify one fission fragment. It is coupled to a  $\Delta E$ -E telescope to select the reaction channel, i.e. the fissioning nucleus (from U to Cf), and to deduce the excitation energy. Mass distribution is obtained with a resolution below 0.8 mass unit (FWHM) and elemental distribution with a resolution around  $\Delta Z/Z=1.5\%$  (FWHM) [15]. For the first time, isotopic yields depending on excitation energy were obtained over the whole fission-fragments range. Nevertheless, the kinematical boost is still too weak for the heavy group, and uncertainties on isotopic yields for the most produced fission fragments of this group are around 20% (statistical) and 10% (systematic).

Accurate measurement of nuclear charge over a large dynamics can only be obtained using inverse kinematics at relativistic energy. At such high energy, ions are fully stripped, thus the ionic charge obtained by energy-loss ( $\Delta E$ ), gives a direct measurement of the nuclear charge ( $Z$ ). The main difficulty lies in the measurement of the mass number since it requires a large-scale detection system to combine the energy-loss measurement of the heavy ion with its time-of-flight (ToF) and its tracking through a magnetic field ( $B\rho$ ). With these three observables, the mass  $A$  of the ion can be deduced using the so-called  $\Delta E$ - $B\rho$ -ToF method, based on the following equation:  $A/Z \propto B\rho/\beta\gamma$ .

This method was already applied in the 90's at GSI in pioneering experiments. In a first type of experiment, one fragment only, produced after fragmentation or fission of primary beam, was identified in mass and charge [16] thanks to the fragment separator (FRS) [17], but with a limited transmission due to the  $\pm 15$  mrad angular acceptance. In a second type of experiments, the FRS was used to select and identify, on an event-by-event basis, secondary radioactive actinide beams, and their fission was induced at its final focal plane by Coulomb excitation. Both fission-fragment charges were measured in coincidence with a good resolution over the whole fragment range [18, 19], but the masses were missing.

The SOFIA experiment comes within the scope of this last experiment. The breakthrough compared to previous experiments, is that the  $\Delta E$ - $B\rho$ -ToF method was applied at two levels: first for the identification of the secondary beam and then, for each fission fragment in coincidence. For this purpose, the experiment can only take place at the GSI facility, the only heavy-ion accelerator to provide and unambiguously identify secondary actinide beams at relativistic energy up to neptunium isotopes. Moreover, the spectrometer was conceived to fit with the already existing ALADIN (A Large Acceptance DIpole magNet) magnet, located at the cave C, mandatory to get the masses of the fission fragments. We will report on results obtained on  $^{234,235,238}\text{U}(\gamma, f)$  from the first experiment in August 2012, and on  $^{236}\text{U}(\gamma, f)$  from extra-shifts performed with an upgraded set-up in October 2014.

## 2 Experimental set-up

### 2.1 Radioactive secondary beam

All secondary actinide beams are produced by fragmentation of  $^{238}\text{U}$  primary beam at 1 A.GeV in a Be target coupled with a Nb stripper. Secondary beams are selected by the FRS operated as a momentum-loss achromat spectrometer [20]. The first two dipoles make a selection in  $B\rho$  and the last two dipoles, in energy loss in the intermediate focal plane degrader. Figure 1 (left) shows the 2014 set-up. Event by event, actinides are identified thanks to a Triple-MUSIC (Multiple Sample Ionization Chamber) to get not only the  $\Delta E$  measurement from the energy loss collected on the anode plane, but also the horizontal angle from the electron drift times. The time of flight is measured by two plastic scintillators, one located at S2 and the other one at cave C. The horizontal measurements are provided at S2 by the scintillator, and at cave C by a MWPC [21]. Figure 1 (right) shows the identification plot for the  $^{236}\text{U}$  setting. It illustrates that the actinides are unambiguously identified and can be selected with a graphical cut.

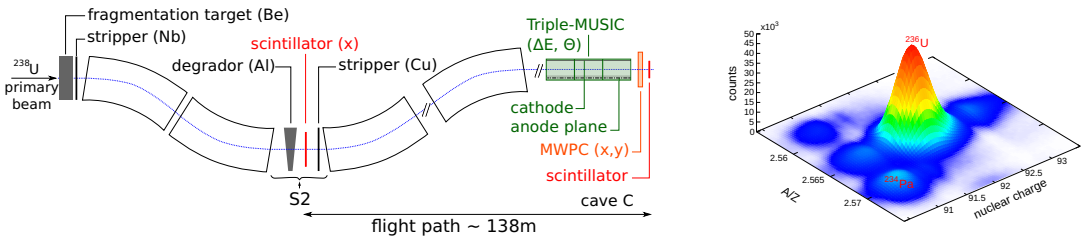


**Figure 1.** Left: schematic view of the FRS and the setup built in October 2014 to apply the  $\Delta E$ - $B\rho$ -ToF method for the secondary-beam identification. Right: Secondary-beam identification for the  $^{236}\text{U}$  FRS setting.

### 2.2 Electromagnetic versus nuclear fission

Depending on the nuclear charge of the target and on the impact parameter, different reaction channels are opened: Nuclear reactions (for small impact parameters) and Coulomb excitations (for high-Z targets and large impact parameters). Coulomb excitation populates the giant dipole resonance (GDR) with an excitation energy around 12 MeV. The excited compound nucleus may decay via fission. As an example, electromagnetic-induced fission of  $^{236}\text{U}$  is a surrogate reaction of 6 MeV neutron induced fission of  $^{235}\text{U}$ . To maximize this low-energy fission induced by Coulomb excitation, high-Z targets are used. Two uranium targets and one lead target are mounted in an active target as cathode

whose principle is detailed in [19], whereas the anodes are made of aluminium foils. In 2014, one more thick aluminium target dedicated to nuclear-fission measurement was mounted into the chamber. The nuclear-induced fission contribution, calculated from fission in anodes and aluminium target, is subtracted at the last stage of the analysis. The number of electromagnetic-induced fissions for the different uranium isotopes is reported in Table 1.

**Table 1.** Statistics for the different electromagnetic-induced fission reactions.

reaction	statistics	year	reaction	statistics	year
$^{234}\text{U}(\gamma, f)$	$1.9 \times 10^5$	2012	$^{236}\text{U}(\gamma, f)$	$2 \times 10^6$	2014
$^{235}\text{U}(\gamma, f)$	$1.1 \times 10^6$	2012	$^{238}\text{U}(\gamma, f)$	$1 \times 10^6$	2012

### 2.3 Fission Fragments

Figure 2 shows on the left side a scheme of the dedicated set-up developed for the ALADIN magnet, and on the right side the results obtained for the nuclear charge (up) and mass (down) distributions. Fission fragments go through a Twin-MUSIC made of two identical MUSICs with a common vertical cathode. Each part has a segmented anode plane in order to provide for each fission fragment its nuclear charge from the energy-loss signals and its horizontal angle from the electron drift times. To complete the tracking, two MWPC detectors [21] located up- and downstream ALADIN give the  $(x, y)$  coordinates. Finally, the time of flight of each fragment is measured between the plastic scintillator located prior to the active target, and the time-of-flight wall [22]. The elemental distribution was measured with a resolution (FWHM) of 0.4 charge unit in 2012 and 0.35 charge unit in 2014. The mass distribution was measured in 2012 with a resolution (FWHM) of 0.6 mass unit in the light fragments group and 0.8 mass unit in the heavy fragments group. Analysis is still in progress for the data taken in 2014.

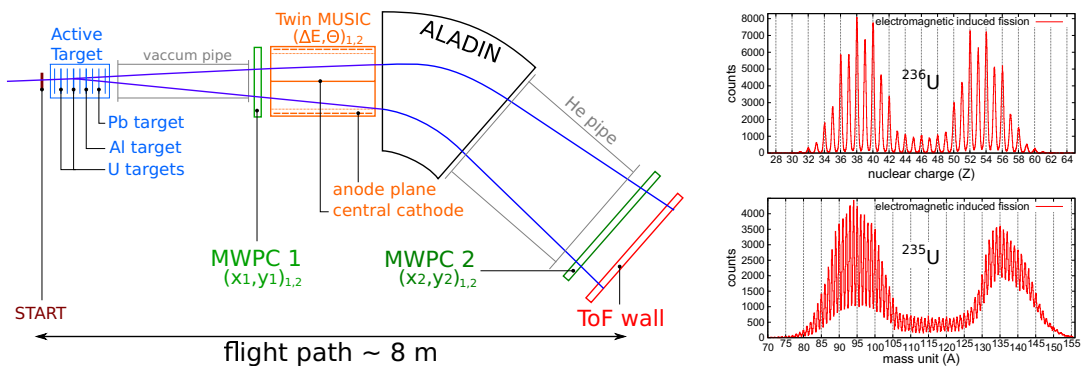


**Figure 2.** Left: schematic drawing of the setup built in October 2014 to apply the  $\Delta E$ - $B\rho$ -ToF method for each fission fragment. Right up: elemental distribution obtained in 2014 for  $^{236}\text{U}(\gamma, f)$  reaction. Right down: mass distribution obtained in 2012 for  $^{235}\text{U}(\gamma, f)$  reaction [23].

### 3 Elemental, isobaric and isotopic fission yields

Yields are calculated from the different distributions. Figure 3 shows the comparison of the experimental results for the elemental yields (left) and mass yields (right) obtained for the  $^{234,235,236,238}\text{U}(\gamma, f)$  reactions. Error bars are reported in the figure. Except for the  $^{234}\text{U}$  case, where the statistics is a factor 10 less than for the  $^{235,236,238}\text{U}$  cases, uncertainties on  $Y(Z)$  and  $Y(A)$  are better than 2 % ( $\sigma$ ) even for the symmetric valley which is less populated. Mass yields are a good probe of the influence of the nascent heavy fission-fragments shell structure in the scission process. Whereas the heavy fragment seems to be stabilized around  $A = 138-140$ , the average mass of the light fragments increases with the mass of the fissioning nuclei. More precisely, the elemental yields show that the standard 1 (ST1) and standard 2 (ST2) asymmetric fission modes [24], have different weights, depending on the mass of the fissioning nucleus. The ST1 mode, characterized by a heavy fragment strongly influenced by the spherical shell gap  $Z=50$ , is predominant for  $^{238}\text{U}$ . Then, for lighter compound nuclei, the ST2 mode, characterized by a heavy fragment strongly influenced by shell effects leading to an enhancement of  $Z=54$ , is more and more populated.

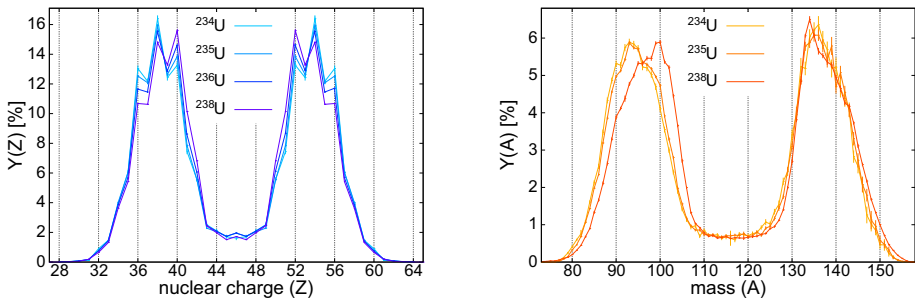


**Figure 3.** Elemental yields (left) and isobaric yields (right) measured for  $^{234,235}\text{U}(\gamma, f)$  [23],  $^{236}\text{U}(\gamma, f)$  and  $^{238}\text{U}(\gamma, f)$  [25].

Figure 4 presents the comparison between the experimental elemental yields for  $^{236}\text{U}(\gamma, f)$  and the JEFF-3.1.1 and BVII-1 evaluated elemental yields for  $^{235}\text{U}(n, f)$  for 3 different neutron-beam energies.

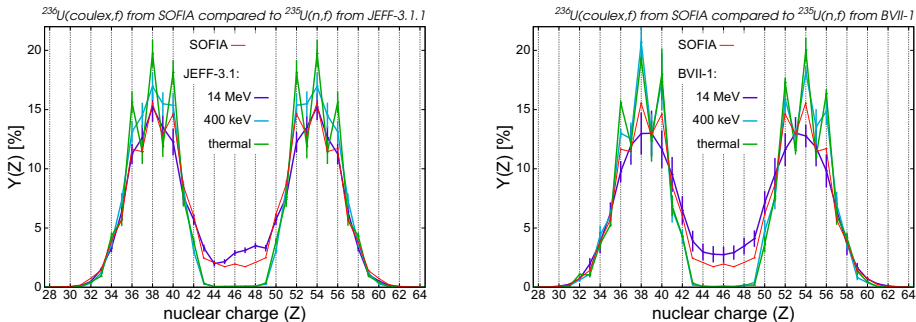


**Figure 4.** Comparison of elemental yields between the experimental data for  $^{236}\text{U}(\gamma, f)$ , and the evaluated data from JEFF-3.1.1 (left) and BVII-1 (right) for  $^{235}\text{U}(n, f)$  reactions for 3 different neutron-beam energies.

As previously underlined, the excitation energy is not measured but is expected to be around 12 MeV in average. With increasing excitation energy, the symmetric valley is more populated, and the even-odd staggering is decreasing. The comparison of the SOFIA experimental data with evaluated data shows that the peak-over-valley ratio is consistent with an excitation energy slightly above 12 MeV, and that the JEFF-3.1.1 evaluated file is underestimating the even-odd staggering for the 400 keV incident neutrons.

Finally, isotopic fission yields obtained for  $^{235}\text{U}(\gamma, f)$  [26] are presented in Fig. 5. The whole fission-fragments dynamics are covered, from  $Z=32$  to  $Z=60$ . Error bars are reported in the figure. For the heavy fission-fragment group and at symmetry, uncertainties are below 7% for the most probable isotopes. At strong asymmetry, always for heavy fission fragments ( $Z \geq 57$ ) uncertainties are below 20%. For the light fission-fragments group, uncertainties are mainly below 2.5%.

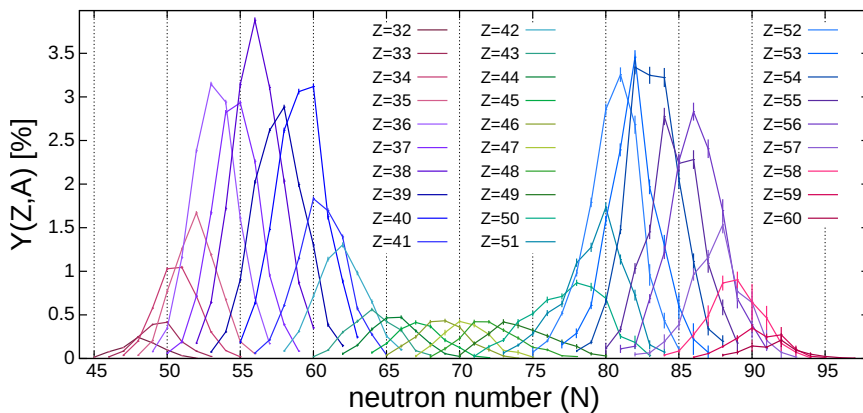


**Figure 5.** Isotopic yields measured for  $^{235}\text{U}(\gamma, f)$  [26].

## 4 Summary and outlooks

Nuclear charge of heavy ions over a large dynamics, up to transuranium nuclei, can only be measured with a good accuracy using inverse kinematics at relativistic energy. This method first used in the 90's at the GSI facility to study fission yields, was recently applied again with a novel experimental set-up, the SOFIA spectrometer. For the first time, the isotopic identification was obtained for both fission fragments in coincidence and for a large range of fissioning nuclei. Fission was induced using Coulomb excitation, with a mean excitation energy around 12 MeV.

For high-statistics data, elemental yields and isobaric yields can be obtained with an uncertainty better than 2%, even for the heavy fission-fragment group, which is the most difficult but most challenging measurement. Even if the excitation energy is not measured, the comparison of the experimental elemental yields with the evaluated files shows that the JEFF-3.1.1 library underestimates the even-odd staggering for the 400 keV neutron-induced fission. Concerning the isotopic fission yields, unprecedented resolution has been reached. For the most produced fission fragments, in the light group, uncertainties are below 2.5%. It is getting a bit worse in the heavy group and at symmetry, but still, it mostly remains below 7%.

Besides the results presented in this proceeding, since the fissioning nuclei and the fission fragments

are unambiguously isotopically identified event by event, the mean neutron multiplicity can be obtained. This can be correlated with the total kinetic energy, which is another observable of the SOFIA experiment. Such results can be found in [26] and will be developed in a further publication [23].

The SOFIA experiment is part of the R<sup>3</sup>B (Reactions with Relativistic Radioactive Beams) [27] research program at the FAIR (Facility for Antiproton and Ion Research) facility. Coupling the SOFIA set-up with standard R<sup>3</sup>B detection systems, new experimental observables will be reachable (see Ref. [26] for more details). Some of these future data will be of high interest for the nuclear-reactor applications, as the neutron multiplicity per fragment and the evolution of the yields with the excitation energy. Finally, if a primary beam of <sup>242</sup>Pu could be produced, accurate fission yields for <sup>238,239</sup>Np, <sup>239,240,241,242</sup>Pu and <sup>241,242</sup>Am fissioning nuclei could be obtained.

## References

- [1] <https://www-nds.iaea.org/exfor/endl.htm>
- [2] A.C Wahl *et al.*, *Proc. 2nd IAEA Symp. on physics and chemistry of fission*, 813 (1969).
- [3] G. Siegert *et al.*, *Phys. Lett. B* **53**, 45 (1974).
- [4] H.G. Clerc *et al.*, *Nucl. Instrum. Methods* **124**, 607 (1975).
- [5] U. Quade *et al.*, *Nucl. Instrum. Methods* **164**, 435 (1979).
- [6] S.I. Mulgin *et al.*, *Nucl. Phys. A* **824**, 1 (2009).
- [7] E. Moll *et al.*, *Nucl. Instrum. Methods* **123**, 615 (1975).
- [8] G. Diiorio and B.W. Wehring, *Nucl. Instrum. Methods* **147**, 487 (1977).
- [9] W. Lang *et al.*, *Nucl. Phys. A* **345**, 34 (1980).
- [10] U. Quade *et al.*, *Nucl. Phys. A* **487**, 1 (1988).
- [11] D. Rochman *et al.*, *Nucl. Phys. A* **710**, 3 (2002).
- [12] A. Bail *et al.*, *Phys. Rev. C* **84**, 034605 (2011).
- [13] C. Rodríguez-Tajes *et al.*, *Phys. Rev. C* **89**, 024614 (2014).
- [14] H. Savajols *et al.*, *Nucl. Instrum. Methods B* **204**, 146 (2003).
- [15] M. Caamaño, O. Delaune *et al.*, *Phys. Rev. C* **88**, 024605 (2013).
- [16] P. Armbruster *et al.*, *Z Phys. A* **355**, 191 (1996).
- [17] H. Geissel *et al.*, *Nucl. Instrum. Methods B* **70**, 286 (1992).
- [18] K.-H. Schmidt *et al.*, *Phys. Lett. B* **325**, 313 (1994).
- [19] K.-H. Schmidt *et al.*, *Nucl. Phys. A* **665**, 221 (2000).
- [20] K.-H. Schmidt *et al.*, *Nucl. Instrum. Methods A* **260**, 287 (1987).
- [21] ALICE collaboration, *J. Phys. G: Nucl. Part. Phys.* **30**, 1517 (2004).
- [22] A. Ebran *et al.*, *Nucl. Instrum. Methods A* **728**, 40 (2013).
- [23] J.-F. Martin *et al.*, in preparation
- [24] U. Brosa, *Phys. Rev. C* **38**, 1944 (1988).
- [25] E. Pellereau *et al.*, in preparation
- [26] J.-F. Martin *et al.*, *Proc. Perspectives on Nuclear Data in the next Decade Workshop* to be published in *Eur. Phys. Jour. Web of Conferences*
- [27] <https://www-alt.gsi.de/forschung/kp/kp2/collaborations/R3B/R3B-TP-Dec05.pdf>



